

Centrality dependence and isospin effect on W^\pm and Z^0 productions in nucleus-nucleus collisions at $\sqrt{s_{NN}} = 5.02$ TeV

Dai-Mei Zhou¹*, Yu-Liang Yan²†, Liang Zheng³, Ming-Rui Zhao², Xiao-Mei Li², Xiao-Ming Zhang¹, Gang Chen³, An-Ke Lei¹, Ya-Qian Zhu¹, Xu Cai¹, and Ben-Hao Sa^{1,2}‡¹

¹ *Key Laboratory of Quark and Lepton Physics (MOE) and Institute of Particle Physics, Central China Normal University, Wuhan 430079, China.*

² *China Institute of Atomic Energy, P. O. Box 275 (10), Beijing, 102413 China.*

³ *School of Mathematics and Physics, China University of Geosciences (Wuhan), Wuhan 430074, China.*

In this paper, the centrality dependent Z^0 and W^\pm production and the isospin effect in W^\pm production are investigated with a parton and hadron cascade model PACIAE in Pb–Pb collisions at $\sqrt{s_{NN}} = 5.02$ TeV. ALICE data of Z^0 production in Pb–Pb collisions at $\sqrt{s_{NN}} = 5.02$ TeV are found to be reproduced fairly well. The prediction on W^\pm production in the same collision system is given as well. An interesting isospin effect is observed in exploring the charge asymmetry between W^+ and W^- as a function of the asymmetry between number of valence u - and d -quarks varied from small to large collision systems at center-of-mass energy 5.02 TeV. The results serve as a important benchmarks for understanding the initial conditions of heavy-ion collisions.

I. INTRODUCTION

W^\pm and Z^0 vector bosons are heavy particles with masses of $m_{W^\pm} = 80.39$ GeV/ c^2 and $m_{Z^0} = 91.19$ GeV/ c^2 [1]. They are mainly produced in the hard partonic scattering processes with large momentum transfer at the early stage of the (ultra-)relativistic nucleus–nucleus collisions. Their main production processes are

$$u\bar{d} \rightarrow W^+, \quad d\bar{u} \rightarrow W^-$$

and

$$u\bar{u} \rightarrow Z^0, \quad d\bar{d} \rightarrow Z^0$$

in the leading order approximation [2]. With the involvement of the valence u - and d -quarks inside the beam particles, the isospin difference between protons and neutrons is important on the production of W^+ and W^- . It is therefore expected that the charge asymmetry between W^+ and W^- is related to the relative abundance of protons or neutrons of the colliding nuclei, irrespective of the collision system size.

In comparison with the evolution time of the heavy-ion collision system, 10 to 100 fm/ c for instance, decay time of W^\pm/Z^0 , which can be estimated with the full decay width Γ [1],

$$t = \frac{\hbar}{\Gamma}, \quad t_{W^\pm} = 0.0922 \text{ fm}/c, \quad t_{Z^0} = 0.0791 \text{ fm}/c,$$

is very short. The W^\pm/Z^0 leptonic decays

$$W^+ \rightarrow l^+\nu_l, \quad Z^0 \rightarrow l^+l^-, \quad (l: e, \mu, \tau)$$

are nearly instantaneous. As the produced leptons weakly interact with the partonic and hadronic matter created in heavy ion collisions, W^\pm and Z^0 , similar as the prompt direct photons, are powerful probes for investigating the properties of the initial stage of the evolving system and the partonic structure of the colliding nuclei.

The measurement of W^\pm/Z^0 production is very important to calibrate the collision geometry information of nuclear collisions and of great experimental interests. Many observables in the heavy ion studies require the knowledge of geometric quantities such as the nuclear thickness function (T_{AA}), the number of participant nucleons (N_{part}), and the number of binary collisions (N_{coll}), which are usually obtained using the Glauber model [3–6]. Without participating the final state interactions, W^\pm/Z^0 bosons are ideal probes to test the validity of collision geometries applied in the experimental analysis.

The CMS and ATLAS Collaborations have first measured W^\pm and Z^0 production in Pb–Pb collisions at $\sqrt{s_{NN}} = 2.76$ TeV [7–10]. Recently, the ALICE and ATLAS Collaborations published the measurements of Z^0 production at forward rapidities [11] and W^\pm/Z^0 production at mid-rapidity [12, 13], in Pb–Pb collisions at $\sqrt{s_{NN}} = 5.02$ TeV, respectively. The W^\pm and Z^0 production cross sections are also measured in p–Pb collisions at $\sqrt{s_{NN}} = 5.02$ by the ALICE and CMS collaborations [14, 15]. All those measurements are declared to be well reproduced by the leading-order (LO) and/or next-to-leading-order (NLO) perturbative Quantum Chromo Dynamics (pQCD) calculations [16–19] using the CT14 Parton Distribution Function (PDF) set [16] with and without the parameterized nuclear modified PDF (nPDF) like EPPS16 [19]. As the experimental data analysis relies strongly on the template calculated with NLO pQCD [20], comparing experimental data to the LO or NLO pQCD predictions only is incomplete. The study of W^\pm/Z^0 production in heavy-ion collisions with Monte-Carlo simulation may provide more differen-

*zhoudm@mail.ccnu.edu.cn

†yanyl@ciae.ac.cn

‡sabh@ciae.ac.cn

TABLE I: Per-event multiplicity of Z^0 and W^\pm bosons in rapidity interval $2.5 < y < 4.0$ for three different centrality classes (0–(%)20), 20–90% and 0–90%) in Pb–Pb collision at $\sqrt{s_{NN}} = 5.02$ TeV.

Centrality	0–20%	0–90%	20–90%
$dN_{Z^0}/dy _{exp.}$	0.996×10^{-7}	0.379×10^{-7}	0.198×10^{-7}
Rescaled $dN_{Z^0}/dy _{exp.}^{**}$	5.03	1.91	1.00
$dN_{Z^0}/dy _{paciae}$	9.92	4.42	2.84
Rescaled $dN_{Z^0}/dy _{paciae}^{**}$	3.50	1.56	1.00
$dN_{W^+}/dy _{paciae}$	4.97	2.23	1.43
Rescaled $dN_{W^+}/dy _{paciae}^{**}$	3.49	1.56	1.00
$dN_{W^-}/dy _{paciae}$	5.30	2.37	1.50
Rescaled $dN_{W^-}/dy _{paciae}^{**}$	3.54	1.58	1.00

* Taken from ALICE [11]

** Rescale to the digital in 20-90% centrality.

tial understandings into the microscopic transport properties of the collision system.

II. MODEL

A parton and hadron cascade model PACIAE [21] is employed to simulate Z^0 production in pp and Pb–Pb

collisions at centre-of-mass energy 5.02 TeV. The results are compared with the ALICE measurements [11]. The W^\pm production is predicted in Pb–Pb collisions at $\sqrt{s_{NN}} = 5.02$ TeV. A systematic analysis of W^\pm charge asymmetry in nucleon–nucleon (NN): pp, pn, np, nn collisions and in nucleus–nucleus (AA): Cu–Cu, Au–Au, Pb–Pb and U–U collisions is also studied.

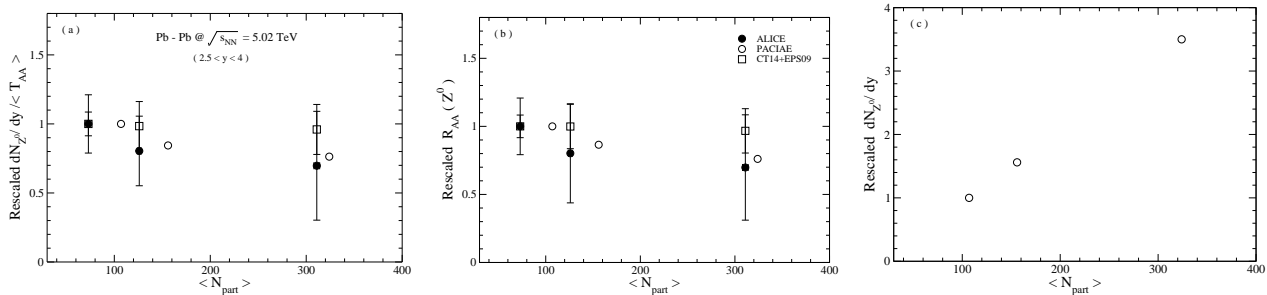


FIG. 1: Centrality dependence on Z^0 production in Pb–Pb collisions at $\sqrt{s_{NN}} = 5.02$ TeV: panel (a) for $dN/dy / \langle T_{AA} \rangle$, (b) for R_{AA} , and (c) for dN/dy .

The PACIAE model is based on PYTHIA event gen-

erator (version 64.28) [22]. For NN collisions, with re-

spect to PYTHIA, the partonic and hadronic rescatterings are introduced before string formation and after the hadronization, respectively. The final hadronic state is developed from the initial partonic hard scattering and

parton showers, followed by parton rescattering, string fragmentation, and hadron rescattering stages. Thus, the PACIAE model provides a multi-stage transport description on the evolution of the collision system.

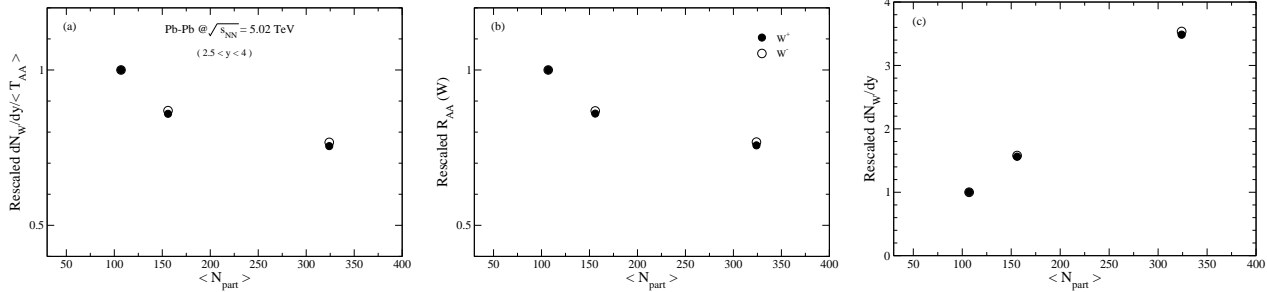


FIG. 2: Centrality dependence on W^\pm productions in Pb–Pb collisions at $\sqrt{s_{NN}} = 5.02$ TeV: panel (a) for $dN/dy / \langle T_{AA} \rangle$, (b) for R_{AA} , and (c) for dN/dy .

For AA collisions, the initial positions of nucleons in the colliding nucleus are sampled according to the Woods-Saxon distribution. Together with the initial momentum setup of $p_x = p_y = 0$ and $p_z = p_{beam}$ for each nucleon, a list containing the initial state of all nucleons in a given AA collision is constructed. A collision happened between two nucleons from different nuclei if their relative transverse distance is less than or equal to the minimum approaching distance: $D \leq \sqrt{\sigma_{NN}^{tot}}/\pi$. The collision time is calculated with the assumption of straight-line trajectories. All such nucleon pairs compose a NN collision time list. A NN collision with least collision time is selected from the list and executed by PYTHIA (PYEVNW subroutine) with the hadronization temporarily turned-off, as well as the strings and diquarks broken-up. The nucleon list and NN collision time list are then updated. A new NN collision with least collision time is selected from the updated NN collision time list and executed with repeating the aforementioned steps till the NN collision list is empty.

With those procedures, the initial partonic state for a AA collision is constructed. Then, the partonic rescatterings are performed, where the LO-pQCD parton-parton cross section [23, 24] is employed. After partonic rescatterings, the string is recovered and then hadronized with the Lund string fragmentation scheme resulting in an intermediate hadronic state. Finally, the system proceeds into the hadronic rescattering stage and produces the final hadronic state observed in the experiments.

The per-event W^\pm/Z^0 production yield is very low, e.g., $dN_{Z^0}/dy \sim 10^{-7}$ at forward-rapidity in the most 20% central Pb–Pb collisions at $\sqrt{s_{NN}} = 5.02$ TeV, as shown in Tab. 1. In this study, the relevant production channels are activated in a user controlled approach by

setting $MSEL = 0$ in PYTHIA together with the following subprocesses switched on:

$$\begin{aligned} f_i \bar{f}_j &\rightarrow W^+/W^- \\ f_i \bar{f}_j &\rightarrow gW^+/W^- \\ f_i \bar{f}_j &\rightarrow \gamma W^+/W^- \\ f_i g &\rightarrow f_k W^+/W^- \\ f_i \bar{f}_j &\rightarrow Z^0 W^+/W^- \\ f_i \bar{f}_i &\rightarrow W^+ W^- \end{aligned}$$

for W^\pm production, and

$$\begin{aligned} f_i \bar{f}_i &\rightarrow \gamma^*/Z^0 \\ f_i \bar{f}_i &\rightarrow g(\gamma^*/Z^0) \\ f_i \bar{f}_i &\rightarrow \gamma(\gamma^*/Z^0) \\ f_i g &\rightarrow f_i(\gamma^*/Z^0) \\ f_i \bar{f}_i &\rightarrow (\gamma^*/Z^0)(\gamma^*/Z^0) \\ f_i \bar{f}_j &\rightarrow Z^0 W^+/W^- \end{aligned}$$

for Z^0 production. In aforementioned equations f refers to fermions (quarks) and its subscript stands for flavor code.

The production of the W^\pm/Z^0 boson is performed using a triggered simulation approach. A normalization factor is needed to account for the trigger bias effect. Unfortunately, this normalization factor is not able obtaining from default PYTHIA run where the W^\pm/Z^0 production subprocesses were not active. The comparison between results using bias sampling technique and experimental data is available investigating trend of the observable only. Therefore we apply a self-normalized

rescaling technique to both of the experimental observables and the model calculations with respect to a reference value at a given argument (such as N_{part} in Fig. 1), as indicated in Tab. 1 and Fig. 1.

As the Quark Gluon Matter and Hadronic Matter are both nearly transparent to the W^\pm/Z^0 bosons, the rescattering of W^\pm/Z^0 bosons are not considered in the partonic and hadronic evolutions in the PACIAE simulations. Thus the results of W^\pm/Z^0 productions from PACIAE simulations are nearly the same as the ones in pQCD for pp collisions.

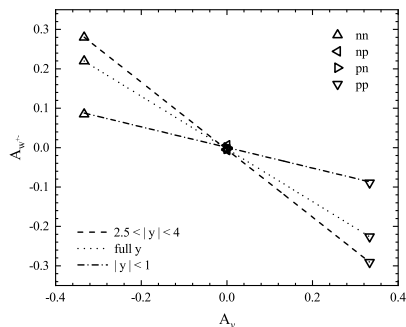


FIG. 3: The correlation between boson (W^\pm) and fermion (valence quark) charge asymmetry in the elementary nuclear-nuclear collisions: n-n (triangle-up); n-p (triangle-left); p-n (triangle-right); p-p (triangle-down) at $\sqrt{s_{NN}}=5.02$ TeV in three symmetrical y intervals: $|y| < 1$, $2.5 < |y| < 4.0$ and full y phase space. The linear fitting are shown for those y intervals as well.

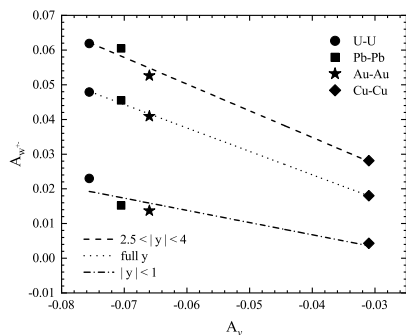


FIG. 4: The correlation between boson (W^\pm) and fermion (valence quark) charge asymmetry in symmetrical nucleus-nucleus collisions: U-U (full circle), Pb-Pb (full square), Au-Au (star), Cu-Cu (full diamond) at $\sqrt{s_{NN}} = 5.02$ TeV in three symmetrical y intervals: $|y| < 1$, $2.5 < |y| < 4.0$ and full y phase space. The linear fitting are shown for those y intervals as well.

III. RESULTS AND DISCUSSIONS

The comparison of the rescaled Z^0 rapidity-differential density $dN_{Z^0}/dy / \langle T_{AA} \rangle$ as a function of N_{part} between PACIAE simulations and the ALICE measurements is

shown on the Fig. 1 panel (a) in Pb-Pb collisions at $\sqrt{s_{NN}} = 5.02$ TeV. In this figure the 0-20% centrality class is the reference point. The panel (a) shows that ALICE measurements [11] are well reproduced by the PACIAE simulations within uncertainties and the centrality dependence is not strong. Similarly, Fig. 1 panel (b) gives the centrality dependence of $R_{AA}(Z^0)$

$$R_{AA} = \frac{1}{\langle N_{\text{coll}} \rangle} \frac{dN/dy|_{\text{PbPb}}}{dN/dy|_{\text{pp}}}. \quad (1)$$

Again, PACIAE simulations agree with the ALICE measurements within errors. It is interesting that the centrality dependence here is nearly the same as the one in panel (a). Finally, Fig. 1 panel (c) is the centrality dependence of dN_{Z^0}/dy . Here the centrality dependence is stronger than the one in panel (a) or (b), as it should be.

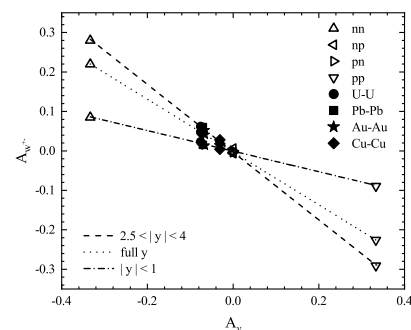


FIG. 5: The correlation between boson (W^\pm) and fermion (valence quark) charge asymmetry in the elementary nuclear-nuclear collisions and symmetrical nucleus-nucleus collisions.

A similar model prediction for W^\pm production in Pb-Pb collisions at $\sqrt{s_{NN}} = 5.02$ TeV is shown in Fig. 2. It is found that the centrality dependence shown in Fig. 2 is quite close to the one in Fig. 1.

The asymmetry between W^+ and W^- productions stemming from the isospin effect can be studied with the W^\pm charge asymmetry

$$A_{W^\pm} = \frac{N_{W^-} - N_{W^+}}{N_{W^-} + N_{W^+}}. \quad (2)$$

as a function of colliding system valence quark charge asymmetry

$$A_v = \frac{N_u - N_d}{N_u + N_d}, \quad (3)$$

where N_u (N_d) stands for the total number of valence u (d) quark in the colliding system.

The correlation between W^\pm and valence quark charge asymmetry in the elementary nucleon-nucleon collisions: n-n (triangle-up), n-p (triangle-left), p-n (triangle-right) and p-p (triangle-down) at $\sqrt{s} = 5.02$ TeV at different y intervals: $|y| < 1$, $2.5 < |y| < 4.0$, and full y phase space are shown in Fig. 3. All those results in

three y intervals can be fitted by a linear function with different slopes. We can also find a feature that the positive correlation flips into negative correlation from n - n to n - p to p - n and to p - p in these three different rapidity intervals. It shows that the slope obtained at mid-rapidity is gentler than that at forward rapidities. This is due to that the isospin effect on W^\pm production is more pronounced at forward rapidities [25].

In Fig. 4 the correlation between W^\pm and valence quark charge asymmetries in minimum bias symmetrical nucleus-nucleus: U-U (full circle), Pb-Pb (full square), Au-Au (star), Cu-Cu (full diamond) collisions at $\sqrt{s} = 5.02$ TeV in three different y intervals: $|y| < 1$, $2.5 < |y| < 4.0$, and full y phase space are given. The linear fitted results are shown as well. Also different y interval has different fitted slope. The valence quark charge asymmetry factor A_ν are all negative, while the W^\pm charge asymmetry factor A_{W^\pm} are all positive, that is to say the correlation have no sign-change from U-U to Pb-Pb to Au-Au and to Cu-Cu collision systems. If we put the data from Fig. 3 and Fig. 4 together, as shown in Fig. 5, we can get very good linear correlations for all collision systems at different y intervals.

IV. SUMMARY

The parton and hadron cascade model PACIAE is employed to simulate the dynamical production of W^\pm and Z^0 bosons in nucleon-nucleon (NN) and nucleus-nucleus (AA) collisions for the first time. The rescaled $dN/dy/\langle T_{AA} \rangle$ and R_{AA} for Z^0 bosons measured by ALICE in p - p and Pb - Pb collisions at centre-of-mass energy 5.02 TeV [11] are reproduced. The correlations between W^\pm charge asymmetry (A_{W^\pm}) and valence u - and d -quark number asymmetry (A_ν) are studied in three rapidity intervals (mid-rapidity $|y| < 1$, forward rapidities $2.5 < |y| < 4$, and the full rapidity region). In each rapidity interval, a linear scaling behavior between A_{W^\pm}

and A_ν is observed by combing the results in different elementary NN (p - p , p - n , n - p and n - n) collision systems. Results obtained from various AA (Cu-Cu, Au-Au, Pb-Pb and U-U) collision systems well follow the scaling established by NN collisions. The nuclear-modified PDF (nPDF) is not adopted in the AA collision setup in this analysis. And the dynamic shadowing on nucleon implemented in PACIAE simulations may affect only the probability of binary collisions in a given AA collision, but not the kinematics of the hard-scattering out-going particles (e.g., W^\pm/Z^0). The universal scaling behavior between A_{W^\pm} and A_ν observed in both NN and AA collision systems hence may provide a vacuum (without the nuclear modification) baseline of the isospin effect on W^\pm production. The nuclear modification on the vacuum nucleon PDF may change the in-going parton kinematics for the hard processes and consequently may impact the p_T - and y -distribution of the out-going particles. This effect may result in a breaking of the A_{W^\pm} - A_ν scaling established in vacuum if looking into a given W^\pm p_T - y phase space. Therefore, by measuring p_T and y differentially, the deviation of the A_{W^\pm} - A_ν correlations between NN and AA systems should provide a new tool to constrain the nPDF in a wide Bjorken- x region. This study serves as a benchmark for the research on the initial conditions of heavy-ion collisions and also sheds light on the understanding of medium-induced higher-order effects on W^\pm/Z^0 production in future works.

Acknowledgments

This work was supported by the National Natural Science Foundation of China (11775094, 11805079, 11905188, 11775313), the Continuous Basic Scientific Research Project (No.WDJC-2019-16) in CIAE, National Key Research and Development Project (2018YFE0104800) and by the 111 project of the foreign expert bureau of China.

-
- [1] Particle data group, Review of Particle Physics, Chinese Phys. C 38 (2014) 27.
 - [2] A. D. Martin, R. G. Roberts, W. J. Stirling and R. S. Thorne, Eur. Phys. J. C 14 (2000) 133, arXiv: hep-ph/9907231 [hep-ph].
 - [3] A. Shor and R. Longacre, Phys. Lett. B 218, 100 (1989).
 - [4] B. I. Abelev, et al., STAR Collaboration, Phys. Rev. C 79, 034909 (2009).
 - [5] B. I. Abelev, et al., ALICE Collaboration, Phys. Rev. C 88, 044909 (2013).
 - [6] D. Miskowiec, <http://www.linux.gsi.de/~misko/overlap/>.
 - [7] CMS Collab., Phys. Lett. B 715 (2012) 66, arXiv: 1205.6334 [hep-ex].
 - [8] ATLAS Collab., Eur. Phys. J. C 75 (2015) 23, arXiv: 1408.4674 [hep-ex].
 - [9] CMS Collab., Phys. Rev. Lett. 106 (2011) 212301, arXiv: 1102.5435 [hep-ex].
 - [10] ATLAS Collab., Phys. Rev. Lett. 110 (2013) 022301, arXiv: 1210.6486 [hep-ex].
 - [11] ALICE Collab., Phys. Lett. B 780 (2018)372, arXiv: 1711.10753v2 [hep-ex].
 - [12] ATLAS Collab., Eur. Phys. J. C 79 (2019) 935, arXiv: 1907.10414v1 [hep-ex].
 - [13] ATLAS Collab., arXiv: 1910.13396v1 [hep-ex].
 - [14] ALICE Collab., JHEP, 02. 077 (2017), arXiv: 1611.03002v2 [hep-ex]; ALICE Collab., arXiv: 2005.11126v1 [hep-ex].
 - [15] CMS Collab., Phys. Lett. B 800 (2020) 135048.
 - [16] S. Dulat, T.-J. Hou, J. Gao, M. Guzzi, J. Huston, P. Nadolsky, J. Pumplin, C. Schmidt, D. Stump, and C. P. Yuan, Phys. Rev. D 93 (2016) 033006, arXiv:1506.07443v2 [hep-ph].
 - [17] K. J. Eskola, H. Paukkunen, and C. A. Salgado, JHEP, 04. 065 (2009), arXiv: 0902.4154 [hep-ph].

- [18] A. Kusina, F. Lyonnet, D. B. Clak, E. Godat, T. Jezo, K. Kovarik, F. I. Olness, I Schienbein, and J. Y. Yu, arXiv: 1610.02925 [nucl-th].
- [19] K. J. Eskola, P. Paakkinen, H. Paukkunen, and C. A. Salgado, *Eur. Phys. J. C* 77 (2017) 163, arXiv: 1612.05741 [hep-ph].
- [20] S. Alioli, P. Nason, C. Oleari, and E. Re, arXiv: 0805.4802v1.
- [21] Ben-Hao Sa, Dai-Mei Zhou, Yu-Liang Yan, Xiao-Mei Li, Shene-Qin Feng, Bao-Guo Dong, and Xu Cai., *Comput. Phys. Commun.* 183, 333 (2012); *ibid*, 224, 412 (2018).
- [22] T. Sjöstrand, S. Mrenna, and P. Skands, *JHEP*, 05, 026 (2006).
- [23] B. L. Combridge, J. Kripfgang, and J. Ranft, *Phys. Lett. B* 70, 234 (1977).
- [24] R. D. Field, *Application of perturbative QCD*, Addison-Wesley Publishing Company, Inc., 1989.
- [25] Zaida Conesa Del Valle, *Performance of the ALICE muon spectrometer. Weak boson production and measurement in heavy-ion collisions at LHC*, Ph. D. thesis: <https://tel.archives-ouvertes.fr/tel-00198703>